J Physiol 591.15 (2013) pp 3765–3776

The Journal of Physiology

Acute failure of action potential conduction in *mdx* muscle reveals a new mechanism of contraction-induced force loss

Jarrod A. Call[1], Gordon L. Warren[2], Mayank Verma[3] and Dawn A. Lowe[1]

[1] *Programs in Rehabilitation Science and Physical Therapy, School of Medicine, University of Minnesota, Minneapolis, MN, USA*
[2] *Department of Physical Therapy, Georgia State University, Atlanta, GA, USA*
[3] *Medical Scientist Training Program, University of Minnesota Medical School, Minneapolis, MN, USA*

Key points

- A primary feature of skeletal muscle lacking the protein dystrophin, as occurring in Duchenne muscular dystrophy, is a hypersensitivity to eccentric contraction-induced injury. Dystrophin is associated with the plasmalemma which in healthy muscle has the physiological function of maintaining resting membrane potential to facilitate action potential generation and conduction during muscle activation.
- We tested the hypothesis that the physiological function of the plasmalemma is impaired as a result of eccentric contractions in dystrophic skeletal muscles.
- Electromyographic analysis of dystrophic muscle from *mdx* mice, the murine model of Duchenne muscular dystrophy, during and immediately after eccentric contractions revealed impairment in the muscle's ability to generate and conduct action potentials.
- In agreement with our electromyographic analysis, assessment of resting membrane potentials showed that dystrophic muscle cells are depolarized immediately after an injurious bout of eccentric contractions.
- Our results suggest a major plasmalemma-based mechanism of strength loss underlying eccentric contraction-induced injury in dystrophic muscle.

Abstract A primary feature of skeletal muscle lacking the protein dystrophin, as occurring in Duchenne muscular dystrophy, is a hypersensitivity to contraction-induced strength loss. We tested the hypothesis that the extensive strength loss results from an impairment in the electrophysiological function of the plasmalemma specifically impaired action potential development. Anterior crural muscles from *mdx* and wildtype mice performed a single bout of 100 electrically stimulated eccentric contractions *in vivo*. Electromyography, specifically the M-wave, was analysed during muscle contraction to assess the ability of the tibialis anterior muscle plasmalemma to generate and conduct action potentials. During eccentric contractions, wildtype mice exhibited a 36% loss in torque about the ankle but *mdx* mice exhibited a greater torque loss of 73% ($P < 0.001$). Despite the loss of torque, there was no reduction in M-wave root mean square (RMS) for wildtype mice, which was in stark contrast to *mdx* mice that had a 55% reduction in M-wave RMS ($P < 0.001$). This impairment resolved within 24 h and coincided with a significant improvement in strength and membrane integrity. Intracellular measurements of resting membrane potential (RMP) in uninjured and injured extensor digitorum longus muscles were made to determine if a chronic depolarization had occurred, which could lead to impaired fibre excitability and/or altered action potential conduction properties. The distributions of RMP were not different between wildtype uninjured and injured muscle cells (median: −73.2 mV *vs.* −72.7 mV, $P = 0.46$) whereas there was a significant difference between *mdx* uninjured and

DOI: 10.1113/jphysiol.2013.254656

injured cells (median: −71.5 mV *vs.* −56.6 mV, $P < 0.001$). These data show that *mdx* muscle fibres are depolarized after an injurious bout of eccentric contractions. These findings (i) suggest a major plasmalemma-based mechanism of strength loss underlying contraction-induced injury in Duchenne muscular dystrophy distinctly different from that for healthy muscle, and (ii) demonstrate dystrophin is critical for maintaining action potential generation and conduction after eccentric contractions.

(Received 13 March 2013; accepted after revision 6 June 2013; first published online 10 June 2013)
Corresponding author J. A. Call: Cardiovascular Research Center, University of Virginia, 409 Lane Avenue, MR4 Building Room 6051, Charlottesville, VA 22903, USA. Email: jac4mt@virginia.edu

Abbreviations ANOVA, analysis of variance; BM, body mass; EBD, Evans blue dye; EDL, extensor digitorum longus; NMJ, neuromuscular junction; RM, repeated measures; RMP, resting membrane potential; RMS, root-mean square; TA, tibialis anterior.

Introduction

Mechanical stress can evoke cell membrane disruption. Specifically, mechanical stress induced by muscle contraction can damage the plasmalemma of muscle fibres, particularly when the cytolinker protein dystrophin is absent (Petrof *et al.* 1993). In this situation, the event becomes pathological and contributes to Duchenne muscular dystrophy. Beyond the plasmalemma's function as a barrier, it is responsible for transmitting action potentials longitudinally along the fibre from the neuromuscular junction to the transverse tubule. A possible impairment of this role has not been thoroughly explored as an initiating mechanism in Duchenne muscular dystrophy pathology. It is well recognized that plasmalemma integrity is compromised when dystrophin is lacking (Ervasti, 2007), but whether this instability is involved in the rapid and large loss of contractility is not known (Petrof *et al.* 1993).

Skeletal muscles lacking dystrophin, such as those from *mdx* mice, exhibit a heightened sensitivity to injury that is induced when a muscle is active as it lengthens (i.e. eccentric contraction-induced injury; Petrof *et al.* 1993; Moens *et al.* 1993). Eccentric contractions can evoke the greatest force production from skeletal muscle, up to twice the force generated during isometric or shortening contractions (Katz, 1939), and therefore these contractions represent a physiologically relevant stress placed on the plasmalemma. Immediately following eccentric contractions, strength losses in *mdx* muscles are 20–60% greater than in normal muscle and this has been shown in isolated fast- and slow-twitch muscles tested *in situ* or *ex vivo* (Brooks, 1998; Lynch *et al.* 2000), as well as in entire muscle groups tested *in vivo* (Call *et al.* 2011). However, we and others have demonstrated that despite greater immediate strength losses following eccentric contractions, *mdx* muscle has a faster strength recovery compared to normal muscle (Brooks, 1998; Call *et al.* 2011).

The difference between normal and *mdx* muscle in the degree of strength loss and subsequent rate of recovery from eccentric contractions provokes the thought that initial causes of injury may be different. The mechanisms of strength loss during and immediately following high-force eccentric contractions have been investigated in normal muscle, with impaired Ca^{2+} release from the sarcoplasmic reticulum thought to play a major role (Balnave & Allen, 1995; Ingalls *et al.* 1998). There is some evidence that the physical disruption of force-generating and/or -transmitting proteins (i.e. contractile and cytoskeletal proteins) also contribute to initial strength decrements in normal muscle (McCully & Faulkner, 1986; Lieber *et al.* 1991), although these contribute to a lesser degree (Warren *et al.* 2001). Because dystrophin is a cytoskeletal structural protein and is implicated in mechanotransduction signalling (Ervasti, 2007), contraction-induced strength loss during and immediately following eccentric contractions may manifest differently in dystrophic compared to normal muscle. Recently, a portion of the strength loss in *mdx* muscle after eccentric contractions has been attributed to myofibrillar impairment (Blaauw *et al.* 2010), with the suggestion that one site of the impairment resides upstream of the contractile apparatus in dystrophic muscle (Lynch *et al.* 2000; Blaauw *et al.* 2010). Other studies have shown that, several minutes to hours after eccentric contractions, there is neuromuscular junction disruption and increased intracellular levels of Ca^{2+} and Na^{+} (Yeung *et al.* 2005; Allen *et al.* 2005; Pratt *et al.* 2013), all of which may indeed be an end result of a cascade of events initiated at the plasmalemma during eccentric contractions.

Dystrophin is associated with the plasmalemma and is thought to contribute to plasmalemmal integrity and the maintenance of intracellular homeostasis. Therefore it is logical that events associated with excitation–contraction coupling at the plasmalemma (i.e. movement of ions and action potential) may be affected by eccentric contractions in dystrophic muscle. It has been shown that dystrophic fibres have depolarized resting membrane potentials (Nagel *et al.* 1990; Carlson & Roshek, 2001; Canato *et al.* 2010; Miles *et al.* 2011) and electromyographic

analysis of non-contracting dystrophic muscle revealed the presence of spontaneous action potentials and complex repetitive discharges (Carter *et al.* 1992; Han *et al.* 2006). These observations suggest that the capacity of dystrophic muscle to maintain the electrochemical gradient necessary for membrane polarization and action potential conduction may be impaired, although there is also evidence demonstrating that dystrophic muscles have normal resting potentials and excitability (Turner *et al.* 1988; Hollingworth *et al.* 1990; De Luca *et al.* 1997; Friedrich *et al.* 2004; Woods *et al.* 2004) making the argument equivocal (Allard, 2006). Nonetheless, eccentric contractions are capable of damaging the plasmalemma of dystrophic muscles as evidenced by the efflux of intracellular enzymes such as creatine kinase and the entrance of impermeant dyes (Petrof *et al.* 1993), and this supports the premise that eccentric contractions may also impair plasmalemmal electrophysiology. However, the consequences of eccentric contractions on excitation–contraction events at the plasmalemma (i.e. action potential propagation) during and in the minutes immediately following eccentric contractions have not been explored in dystrophic muscle.

In our first study, we test the hypothesis that an electrophysiological function of the plasmalemma, specifically action potential conduction, is impaired with high-force contractions and contributes to the exaggerated, immediate strength loss in dystrophic muscle. We utilized an *in vivo* approach to physiologically control muscle contraction via nerve stimulation thereby allowing us to explore mechanisms of initial strength loss downstream of the nerve action potential conduction. Through electromyographic analysis of M-waves, we report a large reduction in the number of fibres conducting action potentials and/or alterations in the fibre action potential conduction properties immediately following repetitive contractions in muscles lacking dystrophin. This impairment resolves within 24 h and coincides with a significant improvement in strength and membrane integrity. In our second study we also demonstrate that resting membrane potential (RMP) in *in vivo*-injured *mdx* muscle cells is altered suggesting that the ability of fibres to depolarize and conduct action potentials is impaired immediately after eccentric contractions. These failures in the electrophysiological functions of the plasmalemma did not occur in muscles of wildtype mice suggesting a novel and unique mechanism of contraction-induced force loss in dystrophic muscle.

Methods

Ethical approval and animal models

Male *mdx* mice (C57Bl/10ScSn-DMD^{mdx}) and wildtype mice (C57Bl/10ScSn) aged 8–10 weeks were purchased from the Jackson Laboratory (Bar Harbor, ME, USA). All mice were housed in groups of 3–4 per cage on a 12 h light/dark cycle. Food and water were provided *ad libitum*. All experiments were initiated when mice were 10 weeks of age. This age was selected to avoid the variability associated with peak cycles of degeneration and regeneration characteristic of *mdx* mice aged 3–8 weeks because the primary objective of this research was to investigate mechanisms of immediate strength loss in dystrophic muscle, not mechanisms of disease onset or pathology. All protocols were approved by the University of Minnesota Institutional Animal Care and Use Committee and complied with guidelines set by the American Physiological Society.

Study I: *in vivo* assessment of strength and M-wave properties before, during, and after injury

Surgical procedure. For surgical implantation of electrodes to record M-waves, wildtype and *mdx* mice ($n = 8$ per genotype) were initially anaesthetized in an induction chamber using isoflurane and electrodes were implanted in the tibialis anterior (TA) muscles of anaesthetized mice as described previously (Warren *et al.* 1998, 1999). Briefly, a 26-gauge needle was passed just beneath the superficial fascial sheath of the TA muscle, at the mid-belly perpendicular to the muscle's longitudinal axis. Deinsulated ends of two platinum–iridium (Pt–Ir) electrode wires (Medwire-Sigmund Cohn Corp. 10Ir9/49T; Mt Vernon, NY, USA) were passed through the needle, and the needle withdrawn so that the wires lay beneath the fascia ∼2 mm apart. This electrode wire spacing permits sampling of M-wave activity from the full thickness of the TA muscle beneath the electrodes (Basmajian & Luca, 1985; Warren *et al.* 1999). The proximal ends of the wires were run subcutaneously to the dorsal cervical region where they could be connected to an EMG amplifier when needed. *In vivo* muscle testing simultaneous with M-wave measurements were initiated 10 days after surgery. The electrode impedance was checked immediately after surgery and prior to each *in vivo* muscle testing. Impedance at 30 Hz was measured and impedance for both wildtype and *mdx* mice remained stable at 10–20 kΩ throughout the study period.

***In vivo* strength measurements and injury protocol.** *In vivo* peak isometric torque of the anterior crural muscles (tibialis anterior, extensor digitorum longus and extensor hallucis longus) was assessed as previously described (Baltgalvis *et al.* 2009; Call *et al.* 2010). Briefly, mice were anaesthetized with fentanyl citrate (0.2 mg (kg body mass (BM))$^{-1}$), droperidol (10 mg (kg BM)$^{-1}$) and diazepam (5 mg (kg BM)$^{-1}$). Then the left hindlimb was depilated and aseptically prepared, the foot was placed in

a foot-plate attached to a servomotor (Model 300B-LR; Aurora Scientific, Aurora, Ontario, Canada), and Pt–Ir electrode wires (Model E2-12; Grass Technologies, West Warwick, RI, USA) were inserted percutaneously on either side of the peroneal nerve. Careful initial placement of the electrodes and constant monitoring of torque tracings were necessary to ensure the electrodes were neither too deep nor too proximal (with reference to the nerve) to cause recruitment of the posterior crural muscles (e.g. gastrocnemius muscle). Contractions were induced via stimulation of the peroneal nerve by a stimulator and stimulus isolation unit (Models S48 and SIU5, respectively; Grass Technologies). Torque and M-wave as a function of stimulation frequency was measured during 10 isometric contractions (150 ms duration) at varying stimulation frequencies (20, 40, 60, 80, 100, 125, 150, 200, 250, 300 Hz) to demonstrate physiological relevancy based on two considerations: (1) hindlimb motor unit recruitment during normal movement, i.e. typical muscle activation in rodents occurs between 60 and 100 Hz (Gorassini *et al.* 2000); and (2) in some cases supra-maximal stimulation frequencies (i.e. >200 Hz) can mask contractile phenotypes, such as in the case of the phenomenon known as low-frequency fatigue (Jones *et al.* 1982). After these measurements of submaximal and maximal isometric torques, the anterior crural muscles were injured by performance of 100 electrically stimulated eccentric contractions. During each eccentric contraction the foot was passively moved from 0 deg (positioned perpendicular to tibia) to 19 deg of dorsiflexion where the anterior crural muscles performed a pre-lengthening 100 ms isometric contraction followed by an additional 50 ms of stimulation while the foot was moved from 19 deg of dorsiflexion to 19 deg of plantarflexion. Each eccentric contraction was separated by 10 s and the entire protocol lasted ∼18 min. A 5 min rest following the eccentric contraction protocol was given prior to assessment of the post-injury torque–stimulation frequency relationship. A separate group of *mdx* mice performed 100 concentric contractions by anterior crural muscles ($n = 4$). This protocol was done similarly to the eccentric contraction except that the foot was passively moved to 19 deg of plantarflexion, then during stimulation it was rotated to 19 deg of dorsiflexion.

M-wave assessments. During *in vivo* strength assessment, the M-wave signal was assessed as previously described (Warren *et al.* 1999). Each M-wave recording was analysed by calculating the root mean square (RMS). RMS was calculated for the full 150 ms of an isometric contraction and the first 100 ms (i.e. the isometric portion) of an eccentric or concentric contraction. Because the anterior crural muscles were maximally recruited via electrical stimulation of the common peroneal nerve, a decrease in M-wave RMS was interpreted as impairment of action potential generation and conduction (Warren *et al.* 1999, 2000). Additionally, M-wave median frequencies were determined from the M-wave signals as previously described (Warren *et al.* 1999); the median frequency determined for a muscle equals the mean value determined for seven M-waves acquired during a 40 Hz isometric stimulation.

Assessment of membrane permeability. Evans blue dye (EBD) uptake into muscle fibres, as described previously (Hamer *et al.* 2002; Wooddell *et al.* 2010), was used to assess membrane permeability and to determine if this coincided with loss of M-wave RMS and recovery of M-wave RMS. Briefly, a solution of 3% EBD (Sigma) at 1.0 ml $(10\ \text{g BM})^{-1}$ was delivered through an intraperitoneal injection in a subset of *mdx* mice. For the 3 h time point, EBD solution was injected 1 h prior to an *in vivo* eccentric-injury protocol and the tissue analysed 3 h after the start of the protocol ($n = 5$). For the 24 h time point, the mice were subjected to the eccentric-injury protocol, EBD injected at 20 h post-injury and muscles dissected 4 h later ($n = 4$).

Study II: *ex vivo* assessment of resting membrane potential

The results from Study I indicated that impaired action potential generation and conduction correlated with a significant portion of the strength loss in dystrophic muscle immediately after contraction-induced injury. In this study, intracellular RMPs were measured in muscles immediately following contraction-induced strength loss to assess the extent of plasmalemmal depolarization, which can affect the ability of muscle fibres to conduct action potentials.

Eccentric contraction-induced injury of the anterior crural muscles in wildtype and *mdx* mice was done *in vivo* as in Study I. Immediately following the post-injury strength assessment, extensor digitorum longus (EDL) muscles were harvested and prepared for measurement of RMP. Due to the nature of insertion of the proximal tendon, the TA muscle is difficult to remove without damaging the fibres, so it was not used in this study. Instead, the EDL muscle was used for this experiment because both proximal and distal tendons are easily accessible and the percentage strength deficit for the EDL muscle measured *ex vivo* is the same as that measured for the entire anterior crural muscle group *in vivo* (Ingalls *et al.* 1998).

Resting membrane potential measurement. Measurement of cell RMP from uninjured and injured EDL muscles of wildtype ($n = 6$) and *mdx* ($n = 8$) mice was done

as previously described (Warren *et al.* 1993). Individual EDL muscles were pinned through the tendons onto a hardened silicone adhesive contained in a Plexiglas chamber filled with circulating Krebs buffer maintained at 25°C and bubbled with 95% O_2–5% CO_2 gas. Glass microelectrodes pulled on a horizontal pipette puller (Sutter Instruments Co., Model P-87, Navato, CA, USA) and filled with 3 M KCl were used. An Ag–AgCl-coated wire was placed in the buffer and served as a reference. RMP was measured with a computer-controlled microelectrode amplifier (MultiClamp 700A, Axon Instruments, Inc., Union City, CA, USA). Microelectrode positioning was controlled with a micromanipulator micropositioning system (Sutter Instruments Co.), and movements of ∼5 μm were made toward the muscle until an abrupt negative voltage deflection occurred on the oscilloscope. Once a deflection had occurred the negative potential was monitored for a 10–15 s period, and then the following movement sequence was performed to ensure the microelectrode was inside a cell and not near or against a membrane: (i) the microelectrode was slowly advanced by increments of 2 μm until the negative deflection reversed (out of the cell), (ii) the microelectrode was then slowly withdrawn by increments of 2 μm to observe the negative deflection again (back into the cell), and (iii) the microelectrode continued a slow withdrawal by increments of 2 μm until the negative deflection again reversed (out of the cell). If a recording did not show this pattern, the microelectrode was withdrawn and moved to another position on the muscle. The recorded RMP was the most negative potential observed while the potential drift was less than ±1 mV over a 5 s period. Only the most superficial fibres were examined because it is difficult to determine the reference voltage for deeper fibres. In each muscle, RMP measurements started at the lateral extreme of the mid-belly and 60 μm movements were made toward the medial extreme between recordings to ensure each measurement was taken from a different cell. Successful recordings were made in ∼25 cells per muscle.

Statistics

For Study I, peak eccentric torque and M-wave RMS during 100 eccentric contractions were analysed by two-way repeated measures (RM) analysis of variance (ANOVA) with repeated measures on the eccentric contraction number (1st contraction through to 100th contraction) and the other factor being mouse strain (wildtype *vs.* *mdx*). Peak isometric torque and peak M-wave RMS pre- and post-injury were analysed by two-way RM ANOVA with repeated measures on torque or M-wave RMS (pre- *vs.* post-injury) and the other factor being mouse strain. Isometric torque and M-wave RMS as a function of stimulation frequency was analysed by two-way RM ANOVA with RM being pre-, post- and 24-h post-injury (*mdx* only) and the other factor being stimulation frequency. When significant interactions or main effects were found, differences were tested with Tukey's *post hoc* tests. Differences in body mass and peak isometric torque prior to injury between wildtype and *mdx* mice were determined by *t* test. For Study II, uninjured and injured wildtype and *mdx* cell RMP distributions failed the Shapiro–Wilk's normality test. Therefore, distributions were compared by performing the non-parametric Mann–Whitney test and data are described by medians. An α level of 0.05 was used for all analyses. All values are means ± SEM unless noted otherwise (i.e. Study II results).

Results

Study I: *in vivo* assessment of strength and M-wave properties before, during and after injury

As previously reported, *mdx* muscle was found to be hypersensitive to eccentric contraction-induced strength loss compared to wildtype muscle (73 ± 3 *vs.* 38 ± 6% reduction in eccentric peak torque; $P < 0.001$; Fig. 1*A*). However, it remains unresolved how dystrophin deficiency produces this effect in *mdx* muscle. Because dystrophin is crucial for plasmalemmal integrity and the plasmalemma plays a key role in muscle activation, analysis of M-wave amplitude was used to assess the effects of eccentric contractions on action potential conduction. During the performance of eccentric contractions, there was no reduction in M-wave RMS for wildtype mice, which was in stark contrast to what was observed in *mdx* mice where there was a 51 ± 3% reduction in M-wave RMS ($P < 0.001$; Fig. 1*A*). Correlation analysis revealed that 96% of the variance in eccentric torque could be explained by the variance in M-wave RMS for *mdx* mice ($P < 0.001$), but for wildtype mice none of the variance in torque could be explained by the variance in M-wave RMS ($r^2 = 0.417$; $P = 0.877$; Fig. 1*B*). Representative peak isometric torque and M-wave *vs.* time tracings produced pre- and post-injury in wildtype and *mdx* mice are shown in Fig. 1*C*. Peak isometric torque 5 min after eccentric contraction-induced injury was decreased compared to pre-injury by 41 ± 2% in wildtype mice ($P < 0.001$) with no reduction in M-wave RMS ($P = 0.955$), and in *mdx* mice, peak isometric torque was 60 ± 5% less than pre-injury ($P < 0.001$), and M-wave RMS was decreased by 39 ± 6% ($P = 0.010$).

To determine if eccentric contractions affected M-wave RMS differently in wildtype and *mdx* mice at less than maximal stimulation frequencies, we simultaneously assessed isometric torque and M-wave RMS as a function of stimulation frequency pre- and post-injury in wildtype and *mdx* mice. There was a significant 3-way

interaction (that is, between genotype × frequency × time) for isometric torque ($P < 0.001$). Isometric torques at stimulation frequencies between 20 and 300 Hz were reduced post-injury compared to pre-injury for wildtype mice (range: −49% to −86%, $P < 0.001$), and *mdx* mice (range: −66% to −85%, $P \leq 0.001$; Fig. 2*A*). Additionally, at stimulation frequencies 150 Hz and greater, *mdx* mice produced a lower post-injury torque as a percentage of pre-injury torque compared to wildtype mice ($P \leq 0.007$; Fig. 2*A*). There was also a significant 3-way interaction between the factors genotype, frequency and time for M-wave RMS ($P < 0.001$). M-wave RMS at each stimulation frequency tested was not affected by eccentric contractions in wildtype mice ($P \geq 0.492$; Fig. 2*B*). In

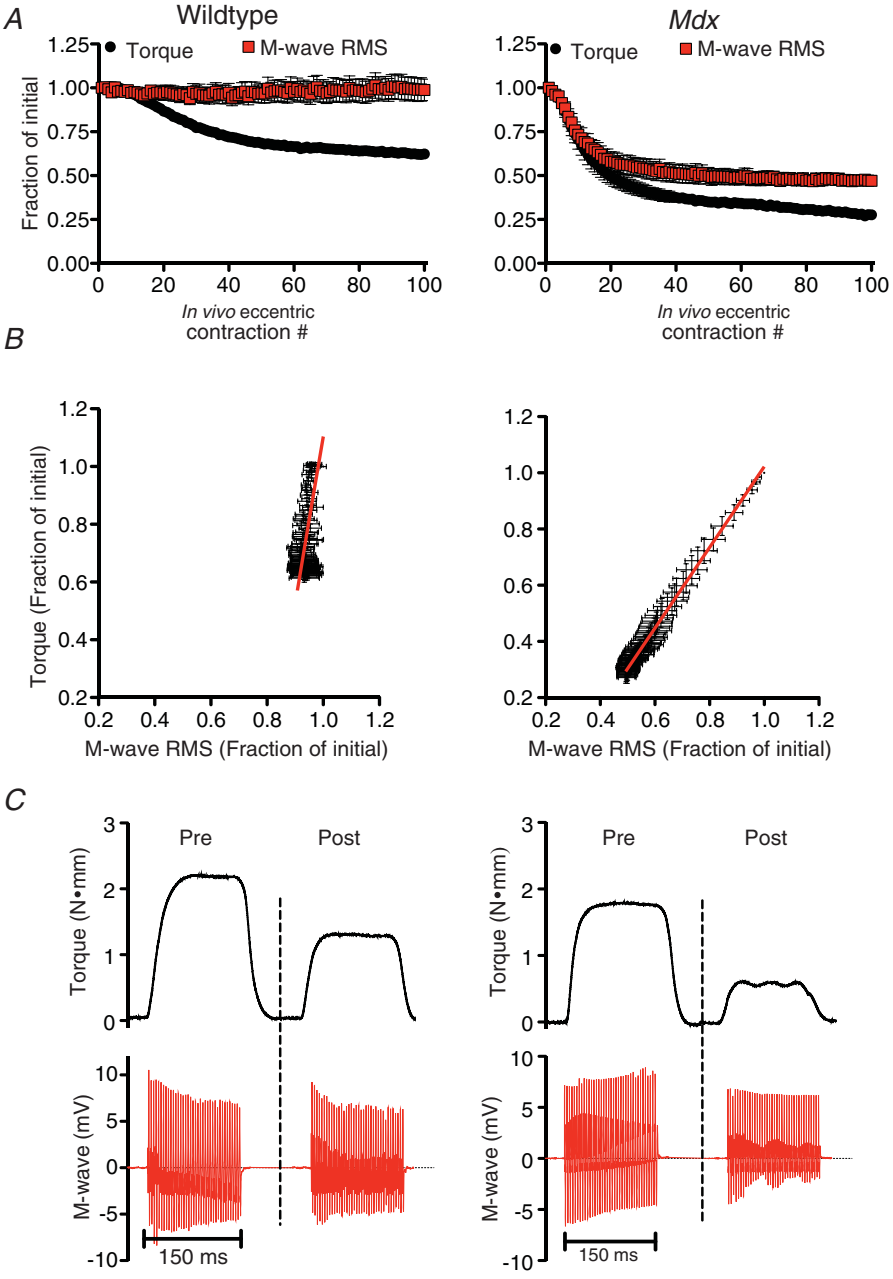

Figure 1. Effect of eccentric contractions on torque and M-wave in wildtype (left) and *mdx* (right) muscle
A, mean ± SEM of eccentric torque during 100 eccentric contractions; mean ± SEM of M-wave RMS during 100 eccentric contractions. Non-visible error bars are contained within the symbols. $n = 8$ per genotype. *B*, correlation analysis of M-wave RMS and peak-eccentric torque from wildtype and *mdx* mice. *C*, representative peak isometric torque and M-wave time tracings produced pre- and post-injury.

contrast, *mdx* mice exhibited a decreased M-wave RMS at stimulation frequencies of 40 Hz and greater, post-injury compared to pre-injury ($P \leq 0.050$; Fig. 2*B*). Also, *mdx* mice had lower M-wave RMS post-injury as a percentage of pre-injury compared to wildtype mice at all stimulation frequencies ($P \leq 0.002$; Fig. 2*B*).

To control for any possible fatiguing effect of the eccentric contraction protocol, a group of *mdx* mice performed 100 concentric contractions with M-wave signal recording. *Mdx* mice that performed 100 concentric contractions showed a small (i.e. 12%) decrease in concentric torque during the protocol (Fig. 3), but 5 min later peak isometric torque and peak M-wave RMS was not different from those produced before the 100 concentric contractions ($P = 0.608$ and $P = 0.927$, respectively; Fig. 3). These results indicate that there is a minimal fatigue element contributing to strength loss in *mdx* mice immediately following the eccentric-injury protocol, and that it is the performance of eccentric contractions that significantly affects M-wave RMS.

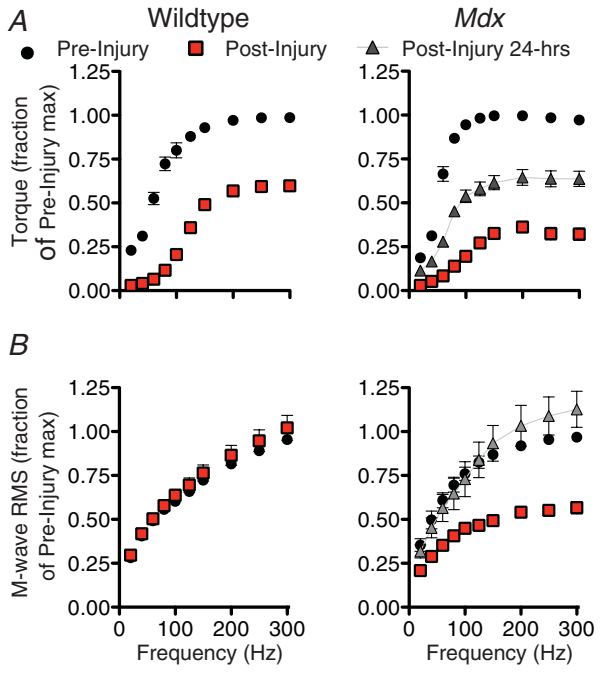

Figure 2. Torque and M-wave RMS as a function of stimulation frequency in wildtype (left) and *mdx* (right) muscle
A, mean ± SEM of isometric torque recorded pre-injury and immediately post-injury for wildtype and *mdx* muscle, and 24 h post-injury (*mdx* only). Post-injury torque at all stimulation frequencies was less than pre-injury torques for wildtype and *mdx*, and *mdx* 24 h. *B*, mean ± SEM of M-wave RMS. M-wave RMS at all stimulation frequencies was not affected by injury among wildtype mice. Conversely, at stimulation frequencies of 40 Hz and greater M-wave RMS was reduced immediate post-injury for *mdx* muscle, and had recovered by 24 h post-injury. Non-visible error bars are contained within the symbol. $n = 8$ per genotype.

We retested *mdx* mice at 24 h after the bout of 100 eccentric contractions to gain insight into whether the cause of the initial reduction in M-wave RMS had a rapid or prolonged repair process. At 24 h post-injury, M-wave RMS was completely recovered at all stimulation frequencies ($P \geq 0.304$; Fig. 2*B*), and isometric torque, while still low relative to pre-injury, was significantly greater at all stimulation frequencies compared to immediately post-injury ($P \leq 0.030$; Fig. 2*A*). At 24 h post-injury, isometric torque at maximal stimulation frequency of 300 Hz had improved from 33% to 63% of pre-injury.

Fast Fourier frequency analysis of individual M-waves was conducted to determine if median frequency was affected immediately following eccentric contractions. The mean median frequencies determined for M-waves acquired pre-, post- and 24 h post-injury are shown in Fig. 4*A*. M-wave median frequency was not different between wildtype and *mdx* muscle ($P = 0.456$) and was not affected by the performance of eccentric contractions (Pre *vs.* Post, $P = 0.135$).

Assessment of M-wave RMS and median frequency provides an evaluation of plasmalemmal functional integrity. Application of normally membrane-impermeant dyes such as EBD can be used to histologically assess plasmalemmal integrity. We analysed EBD uptake in TA muscles from *mdx* mice that performed 100 eccentric contractions at 3 and 24 h post-injury. On average, there

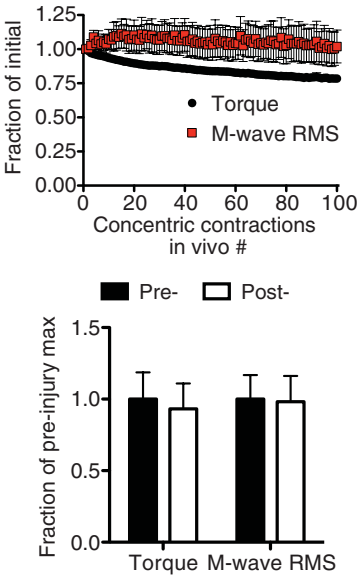

Figure 3. Concentric contractions by anterior crural muscles of *mdx* mice had no effect on peak-concentric torque or TA M-wave RMS
Top, means ± SEM of concentric torque and M-wave RMS produced during 100 concentric contractions. Bottom, peak isometric torque and M-wave RMS 5 min after 100 concentric contractions (Post-) were not different from those before (Pre-). $n = 4$.

were 75% fewer myofibres positively stained at 24 h *vs.* 3 h post-injury ($P = 0.010$; Fig. 4*B*), indicating that the barrier function of the plasmalemma was mostly restored by 24 h post-injury consistent with recovery of plasmalemmal electrophysiological function at that time.

Study II: *ex vivo* assessment of resting membrane potential

Figure 5 illustrates the RMP distribution for all cells measured in uninjured and injured EDL muscles of wildtype and *mdx* mice. There was no difference in the distribution of cell RMP between wildtype uninjured and injured muscles ($P = 0.484$), but a significant difference did exist between *mdx* uninjured and injured muscles ($P < 0.001$). The median RMPs for wildtype uninjured and injured were −73.2 and −72.7 mV, respectively, and the median RMPs for *mdx* uninjured and injured were −71.5 and −56.6 mV, respectively. A small but significant difference in the distribution of cell RMP was also detected between uninjured wildtype and *mdx* muscles ($P = 0.004$). There was no difference between Studies I and II with regard to the strength loss by wildtype and *mdx* mice after eccentric contraction-induced injury.

Discussion

We, and others, have reported that the susceptibility to contraction-induced injury (i.e. strength loss) of *mdx* muscle is greater than that of wildtype muscle, but paradoxically recovers faster (Brooks, 1998; Call *et al.* 2011). We postulated that this dissociation was due to a difference in initiating mechanism of muscle injury. Investigation of normal muscle immediately following eccentric contractions has shown that ∼75% of the strength loss is due to impaired Ca^{2+} release from the SR and the remaining 25% is due to physical disruption of force-generating and force-transmitting proteins (Warren *et al.* 2001). Our data reveal that in *mdx* muscle, approximately half of the immediate strength loss can be attributed to failed action potential generation and/or conduction supporting the premise that the initial causes of contraction-induced strength loss are very different in *mdx* muscle compared to normal muscle. This is important to realize because the susceptibility of *mdx* mouse muscle to eccentric contraction-induced injury has become a standard assessment tool for evaluating therapeutic strategies for muscular dystrophies.

We show that M-wave RMS and muscle cell RMP are not affected by the performance of 100 eccentric contractions in muscles with functional dystrophin (Figs 1 and 5), in concurrence with previous studies on wildtype mice (Warren *et al.* 1993, 1999). Muscle contraction is contingent on proper execution of excitation–contraction processes, and our data demonstrate a major contribution of impaired action potential generation and/or conduction to strength loss in *mdx* muscle immediately following eccentric contractions elicited *in vivo*. For example, *mdx* muscle reductions in peak isometric torque immediately after injury were accompanied by reductions in peak isometric M-wave RMS (Fig. 2). *Mdx* muscle exhibited a rapid and complete recovery of M-wave RMS within 24 h post-injury and this corresponded with a significant improvement in isometric torque at all stimulation frequencies (Fig. 2).

We considered whether or not fatigue potentially caused by the eccentric contraction protocol could have affected

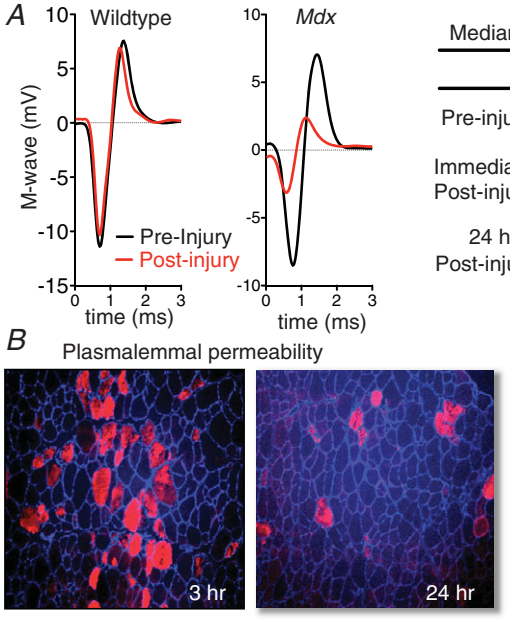

Median Frequency (Hz)	Wildtype	*Mdx*
Pre-injury	1255±15	1211±27
Immediately Post-injury	1402±7	1258±14
24 hr Post-injury	-	1268±12

Figure 4. Plasmalemmal function of *mdx* muscle after injury
A, representative M-wave tracings during isometric contractions assessed pre- and post-injury used to calculate M-wave median frequency. The reduction in the M-wave amplitude in *mdx* muscle mirrors the observations in M-wave RMS. Table: median frequency values are mean ± SEM. $n = 8$ per genotype for Pre-injury and Immediately Post-injury. $n = 5$, *mdx* only for 24 h post-injury. '-' not measured. *B*, EBD permeability of *mdx* myofibres from TA muscles after eccentric contraction-induced injury. Representative images of TA myofibres 3 and 24 h after injury. Horizontal lines represent means ± SEM. *Significantly different from 3 h.

the M-wave signal. Mice that performed 100 concentric contractions (considered non-injurious) of the anterior crural muscles did exhibit a small (∼12%) reduction in concentric torque during the protocol, but peak isometric torque 5 min after the protocol was not different from peak isometric torque prior to the bout of concentric contractions (Fig. 3). More importantly, there was no reduction in M-wave RMS during 100 concentric contractions supporting the idea that it is the performance of eccentric contractions that is injurious to dystrophic muscle and detrimentally affects action potential conduction (Fig. 1). We also considered there might be a contamination of the M-wave signal by stimulation artifact. In preliminary analyses on wildtype and *mdx* mice we tested the extent to which M-wave RMS would reflect changes in stimulation voltage applied to the peroneal nerve. In both *mdx* and wildtype mice, M-wave RMS plateaued after a given stimulation voltage (typically 6–8 V) and subsequently M-wave RMS was not altered when voltage was further increased. This argues against stimulation artifact being a major contaminant in the M-wave signal.

Because we controlled muscle contraction via nerve stimulation we considered the possibility that decrements in M-wave RMS might reflect damage to the neuromuscular junction (NMJ) and we cannot completely rule out this possibility. Pratt and co-workers reported altered EMG characteristics as well as discontinuous and dispersed NMJ morphology in quadriceps muscles of *mdx* but not wildtype mice 24 h following eccentric contraction-induced injury of that muscle (Pratt *et al.* 2013). Theoretically, altered morphology of the NMJ could have contributed to the strength loss and decreased M-wave RMS in our study but this seems unlikely because the decrements we observed occurred during and immediately (<1 h) after the bout of eccentric contractions. In other words, there is no evidence for immediate mechanical disruption of the NMJ during eccentric contractions which would have abruptly impacted strength development. The possibility that NMJ morphology is affected by a slower degradation process initiated by plasmalemmal damage several hours later should be investigated.

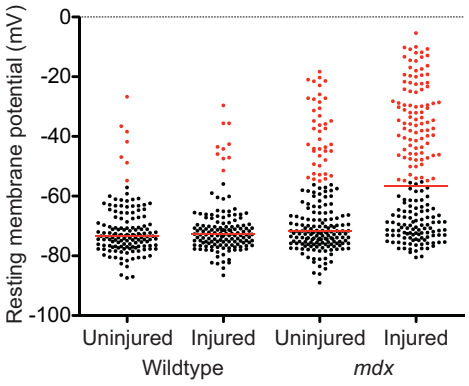

Figure 5. Effect of contraction-induced injury on resting membrane potential
Each dot represents an individual cell sampled from EDL muscles of uninjured and injured wildtype and *mdx* mice. The red bar within each distribution represents the median RMP. Red dots are cells with RMP above –55 mV and black dots are cells with RMP below −55 mV. The total number of cells are: 140, Wildtype Uninjured; 141, Wildtype Injured; 192, *mdx* Uninjured; 196, *mdx* Injured.

Our M-wave frequency analysis (Fig. 4) suggests that no major alterations occurred in fibre action potential conduction properties for either wildtype or *mdx* mice as a result of eccentric contraction-induced injury. M-wave analysis is an imperfect tool for precisely examining action potential properties, and there are reports of non-linear relationships between M-wave activity and muscle force (particularly with the use of surface electrodes; Woods & Bigland-Ritchie, 1983). However, our electrode placement allowed sampling of M-wave activity from the full thickness of the TA muscle beneath the electrodes (Warren *et al.* 1999) and what we observed was a strong linear relationship between muscle torque and M-wave activity during the eccentric contraction protocol (Fig. 1*B*).

A decrease in M-wave RMS (as seen in *mdx*) with no change in M-wave median frequency probably reflects a reduced number of fibres generating or conducting action potentials, and therefore a reduced number of fibres that were activated and contributing to muscle strength development. Data from Study II support this contention showing a significant number of depolarized muscle cells that resulted from contraction-induced injury in *mdx* but not wildtype mice (Fig. 5). A modest depolarization can inhibit a muscle cell's ability to initiate and conduct action potentials, rendering cells inexcitable. Muscle cells depolarized above −55 mV retain only 4% or less of maximal force production (Renaud & Light, 1992; Cairns *et al.* 1995, 1997). We performed a χ^2 analysis to compare percentages of excitable and inexcitable cells using −55 mV to distinguish between the two. We found RMPs more positive than −55 mV in almost 50% of dystrophic muscle cells sampled immediately after injury compared to only 7% in wildtype ($P < 0.001$, Fig. 5; RMPs indicated by red dots). This immediate post-injury time point corresponds to the time when strength reduction is ∼60% and there is a 40% decrease in M-wave RMS. The cells in injured dystrophic muscle with RMP > −55 mV are unlikely to be able to contribute to force development by the muscle, indicating that sustained depolarization is a significant mechanism for eccentric contraction-induced strength loss in dystrophic muscle.

The aetiology of inexcitable cells in dystrophic muscle that is not intentionally injured by eccentric contractions is not clear. Others have shown variable data on the extent to which the absence of dystrophin affects plasmalemmal elements responsible for maintaining

RMP and fibre excitability in uninjured *mdx* muscle (e.g. voltage-gated sodium channels, voltage-gated calcium channels, potassium channels; reviewed in Allard, 2006). What is better established for *mdx* muscle is that following eccentric contractions, injured dystrophin-deficient myofibres demonstrate exaggerated plasmalemmal permeability as shown by dye uptake (Petrof *et al.* 1993). Therefore, impaired M-wave RMS after eccentric contractions (Fig. 1) is probably caused in part by increased membrane permeability and subsequent disturbance in the electrochemical gradient. However, the extent of electrical dysfunction and force loss far exceeds the percentage of plasmalemmal damaged, dye-containing fibres following eccentric contractions (Fig. 4 and Petrof *et al.* 1993), so additional mechanisms must be in play. A leading molecular candidate contributing to plasmalemma impairment in dystrophic muscle is stretch-activated ion channels, which in non-dystrophic muscle have been implicated in membrane depolarization following eccentric contractions (McBride *et al.* 2000). Interestingly, in the study by McBride and co-workers, when stretch-activated channels were blocked, membrane depolarization by eccentric contractions was prevented but the strength loss observed 2 days later was not affected. In *mdx* muscle, blocking stretch-activated ion channels during contractions blunts force loss in flexor digitorum brevis and lumbrical muscles (Yeung *et al.* 2005; Ng *et al.* 2008) and EDL muscles 30 min following eccentric contractions (Whitehead *et al.* 2006), but has no effect on force loss in EDL muscles during eccentric contractions (Baltgalvis *et al.* 2011). In addition to stretch-activated ion channels, sodium channels and the intracellular sodium concentration of *mdx* fibres are perturbed and are associated with altered RMP (Hirn *et al.* 2008), and mechano-sensitive microtubules can enhance intracellular signalling associated with increased plasmalemmal permeability (Khairallah *et al.* 2012). Thus, it is probable that multiple plasmalemma-associated proteins and processes are disturbed in *mdx* muscle during and immediately following eccentric contraction and contribute to plasmalemma electrical dysfunction. It is worth considering what might result if a therapeutic treatment were to correct for the electrical dysfunction; that is, would continued excitation of dystrophin-deficient fibres lessen the strength loss from eccentric contractions, or would it exacerbate strength loss due to failure of another process required for force generation?

The recovery of M-wave RMS at 24 h post-injury (Fig. 2) coincided with a lower percentage of *mdx* fibres containing EBD relative to muscles examined 3 h post-injury (Fig. 4). For this experiment, fibres were exposed to EBD for only 4 h, with EBD induction either at 1 h prior to injury or 20 h post-injury. EBD is non-specific in terms of mechanism of fibre damage, so this association between the recovery of M-wave RMS and fewer fibres positive for EBD at 24 h post-injury does not indicate a cause and effect relationship. However, we and others have demonstrated that injured *mdx* muscle is able to rapidly regain a significant portion of its force-generating capacity (Brooks, 1998; Call *et al.* 2011) suggesting *mdx* muscle has the capability to promptly repair the plasmalemma and electrochemical gradient. Interestingly, the absence of both dystrophin and dysferlin, a Ca^{2+}-sensitive protein critical for membrane repair and sealing (Han, 2011), slows the rapid recovery of dystrophic muscle after eccentric contraction-induced injury (Han *et al.* 2011). Similar to dystrophic muscle, eccentric contractions by muscle of aged rodents also resulted in prolonged depolarization of the RMP, which was attributed to plasmalemma damage (McBride, 2000). Collectively, these results support our finding that the decrement and recovery of M-wave RMS and muscle strength are linked to the impairment and restoration of plasmalemmal excitability, respectively.

Complete recovery of M-wave RMS at 24 h post-injury corresponded to strength increasing from 33% to 63% of the peak isometric torque measured pre-injury (Fig. 2) which suggests that approximately half of the immediate strength loss in *mdx* muscle following eccentric contractions is caused by impaired action potential conduction. These results complement a recent report that myofibrillar disruption causes roughly one-quarter of the strength loss in *mdx* muscle (Blaauw *et al.* 2010). In that study, strength loss was induced *in vivo* via eccentric contractions by gastrocnemius muscles from *mdx* and wildtype mice. Permeabilized fibres from those injured muscles as well as from uninjured muscles were then analysed for Ca^{2+}-activated force, thus bypassing all plasmalemmal and transverse-tubular events in initiating contraction. Fibres from the *in vivo* injured dystrophic muscle produced 28% less force than those from uninjured dystrophic muscle. Those results indicate that the function of the contractile apparatus in dystrophic muscle is affected by eccentric contractions elicited *in vivo* and contributes to immediate force loss. Ca^{2+} homeostasis is disrupted following eccentric contractions, and increased intracellular Ca^{2+} in dystrophic myofibres probably contributes to strength loss by activating calpains and causing Ca^{2+}-directed post-translational modifications (Yeung *et al.* 2005; Allen *et al.* 2005). However, these events would presumably contribute to functional deficits in the time frame of several minutes to hours to days post-eccentric contractions, not immediately. Similarly, events such as inflammation and fibrosis that result from contraction-induced injury contribute to strength deficits in *mdx* muscle but would do so even later, not during and immediately following the contractile activity. Our results reveal a more immediate and proximal mechanism of strength loss in *mdx* muscle, that is, failed action potential generation and/or conduction as a result of muscle cells becoming depolarized and inexcitable.

In conclusion, this is the first evidence of impaired excitability at the plasmalemma as a physiological consequence of performing eccentric contractions in muscle lacking dystrophin. Action potential conduction is necessary for muscle activation and we show that dystrophin appears to be critical for maintaining this process during high-force eccentric contractions. These results help explain the exaggerated strength loss of dystrophic muscle to eccentric contraction-induced injury (Fig. 1) and give insight into dystrophic muscle's rapid recovery of strength. This mechanism of contraction-induced strength loss in dystrophin-deficient muscle represents a distinct difference from that in normal, healthy muscle.

References

Allard B (2006). Sarcolemmal ion channels in dystrophin-deficient skeletal muscle fibres. *J Muscle Res Cell Motil* **27**, 367–373.

Allen DG, Whitehead NP & Yeung EW (2005). Mechanisms of stretch-induced muscle damage in normal and dystrophic muscle: role of ionic changes. *J Physiol* **567**, 723–735.

Balnave CD & Allen DG (1995). Intracellular calcium and force in single mouse muscle fibres following repeated contractions with stretch. *J Physiol* **488**, 25–36.

Baltgalvis KA, Call JA, Nikas JB & Lowe DA (2009). Effects of prednisolone on skeletal muscle contractility in *mdx* mice. *Muscle Nerve* **40**, 443–454.

Baltgalvis KA, Jaeger MA, Fitzsimons DP, Thayer SA, Lowe DA & Ervasti JM (2011). Transgenic overexpression of γ-cytoplasmic actin protects against eccentric contraction-induced force loss in *mdx* mice. *Skeletal Muscle* **1**, 32.

Basmajian JV & De Luca CJ (1985). *Muscles Alive: Their Functions Revealed by Electromyography*. Williams & Wilkins.

Blaauw B, Agatea L, Toniolo L, Canato M, Quarta M, Dyar KA, Danieli-Betto D, Betto R, Schiaffino S & Reggiani C (2010). Eccentric contractions lead to myofibrillar dysfunction in muscular dystrophy. *J Appl Physiol* **108**, 105–111.

Brooks SV (1998). Rapid recovery following contraction-induced injury to in situ skeletal muscles in *mdx* mice. *J Muscle Res Cell* **19**, 179–187.

Cairns SP, Flatman JA & Clausen T (1995). Relation between extracellular $[K^+]$, membrane potential and contraction in rat soleus muscle: modulation by the Na^+-K^+ pump. *Pflugers Arch* **430**, 909–915.

Cairns SP, Hing WA, Slack JR, Mills RG & Loiselle DS (1997). Different effects of raised $[K^+]_o$ on membrane potential and contraction in mouse fast- and slow-twitch muscle. *Am J Physiol Cell Physiol* **273**, C598–C611.

Call JA, Eckhoff MD, Baltgalvis KA, Warren GL & Lowe DA (2011). Adaptive strength gains in dystrophic muscle exposed to repeated bouts of eccentric contraction. *J Appl Physiol* **111**, 1768–1777.

Call JA, McKeehen JN, Novotny SA & Lowe DA (2010). Progressive resistance voluntary wheel running in the *mdx* mouse. *Muscle Nerve* **42**, 871–880.

Canato M, Dal Maschio M, Sbrana F, Raiteri R, Reggiani C, Vassanelli S & Megighian A (2010). Mechanical and electrophysiological properties of the sarcolemma of muscle fibers in two murine models of muscle dystrophy: Col6a1–/– and mdx. *J Biomed Biotechnol* **2010**, DOI: 10.1155/2010/981945.

Carlson CG & Roshek DM (2001). Adult dystrophic (mdx) endplates exhibit reduced quantal size and enhanced quantal variation. *Pflugers Arch* **442**, 369–375.

Carter GT, Longley KJ & Entrikin RK (1992). Electromyographic and nerve conduction studies in the mdx mouse. *Am J Phys Med Rehabil* **71**, 2–5.

Ervasti JM (2007). Dystrophin, its interactions with other proteins, and implications for muscular dystrophy. *Biochim Biophys Acta* **1772**, 108–117.

Friedrich O, Both M, Gillis JM, Chamberlain JS & Fink RHA (2004). Mini-dystrophin restores L-type calcium currents in skeletal muscle of transgenic *mdx* mice. *J Physiol* **555**, 251–265.

Hamer PW, McGeachie JM, Davies MJ & Grounds MD (2002). Evans Blue Dye as an *in vivo* marker of myofibre damage: optimising parameters for detecting initial myofibre membrane permeability. *J Anat* **200**, 69–79.

Han JJ, Carter GT, Ra JJ, Abresch RT, Chamberlain JS & Robinson LR (2006). Electromyographic studies in *mdx* and wild-type C57 mice. *Muscle Nerve* **33**, 208–214.

Han R (2011). Muscle membrane repair and inflammatory attack in dysferlinopathy. *Skelet Muscle* **1**, 10.

Han R, Rader EP, Levy JR, Bansal D & Campbell KP (2011). Dystrophin deficiency exacerbates skeletal muscle pathology in dysferlin-null mice. *Skelet Muscle* **1**, 35.

Hirn C, Shapovalov G, Petermann O, Roulet E & Ruegg UT (2008). $Na_v1.4$ deregulation in dystrophic skeletal muscle leads to Na^+ overload and enhanced cell death. *J Gen Physiol* **132**, 199–208.

Hollingworth S, Marshall MW & Robson E (1990). Excitation contraction coupling in normal and mdx mice. *Muscle Nerve* **13**, 16–20.

Gorassini M, Eken T, Bennett DJ, Kiehn O & Hultborn H (2000). Activity of hindlimb motor units during locomotion in the conscious rat. *J Neurophysiol* **83**, 2002–2011.

Ingalls CP, Warren GL, Williams JH, Ward CW & Armstrong RB (1998). E-C coupling failure in mouse EDL muscle after in vivo eccentric contractions. *J Appl Physiol* **85**, 58–67.

Jones DA, Howell S, Roussos C & Edwards RH (1982). Low-frequency fatigue in isolated skeletal muscles and the effects of methylxanthines. *Clin Sci (Lond)* **63**, 161–167.

Katz B (1939). The relation between force and speed in muscular contraction. *J Physiol* **96**, 45–64.

Khairallah RJ, Shi G, Sbrana F, Prosser BL, Borroto C, Mazaitis MJ, Hoffman EP, Mahurkar A, Sachs F, Sun Y, Chen YW, Raiteri R, Lederer WJ, Dorsey SG & Ward CW (2012). Microtubules underlie dysfunction in Duchenne muscular dystrophy. *Sci Signal* **5**, ra56.

Lieber RL, Woodburn TM & Fridén J (1991). Muscle damage induced by eccentric contractions of 25% strain. *J Appl Physiol* **70**, 2498–2507.

De Luca A, Pierno S & Camerino DC (1997). Electrical properties of diaphragm and EDL muscles during the life of dystrophic mice. *Am J Physiol Cell Physiol* **272**, C333–C340.

Lynch GS, Rafael JA, Chamberlain JS & Faulkner JA (2000). Contraction-induced injury to single permeabilized muscle fibers from *mdx*, transgenic *mdx*, and control mice. *Am J Physiol Cell Physiol* **279**, C1290–C1294.

McBride T (2000). Increased depolarization, prolonged recovery and reduced adaptation of the resting membrane potential in aged rat skeletal muscles following eccentric contractions. *Mech Ageing Dev* **115**, 127–138.

McBride TA, Stockert BW, Gorin FA & Carlsen RC (2000). Stretch-activated ion channels contribute to membrane depolarization after eccentric contractions. *J Appl Physiol* **88**, 91–101.

McCully KK & Faulkner JA (1986). Characteristics of lengthening contractions associated with injury to skeletal muscle fibers. *J Appl Physiol* **61**, 293–299.

Miles MT, Cottey E, Cottey A, Stefanski C & Carlson CG (2011). Reduced resting potentials in dystrophic (mdx) muscle fibers are secondary to NF-κB-dependent negative modulation of ouabain sensitive Na^+-K^+ pump activity. *J Neurol Sci* **303**, 53–60.

Moens P, Baatsen PH & Maréchal G (1993). Increased susceptibility of EDL muscles from mdx mice to damage induced by contractions with stretch. *J Mus Res Cell Motil* **14**, 446–451.

Nagel A, Lehmann-Horn F & Engel AG (1990). Neuromuscular transmission in the mdx mouse. *Muscle Nerve* **13**, 742–749.

Ng R, Metzger JM, Claflin DR & Faulkner JA (2008). Poloxamer 188 reduces the contraction-induced force decline in lumbrical muscles from *mdx* mice. *Am J Physiol Cell Physiol* **295**, C146–C150.

Petrof BJ, Shrager JB, Stedman HH, Kelly AM & Sweeney HL (1993). Dystrophin protects the sarcolemma from stresses developed during muscle contraction. *Proc Natl Acad Sci U S A* **90**, 3710–3714.

Pratt SJP, Shah SB, Ward CW, Inacio MP, Stains JP & Lovering RM (2013). Effects of *in vivo* injury on the neuromuscular junction in healthy and dystrophic muscles. *J Physiol* **591**, 559–570.

Renaud JM & Light P (1992). Effects of K^+ on the twitch and tetanic contraction in the sartorius muscle of the frog, *Rana pipiens*. Implication for fatigue in vivo. *Can J Physiol Pharmacol* **70**, 1236–1246.

Turner PR, Westwood T, Regen CM & Steinhardt RA (1988). Increased protein degradation results from elevated free calcium levels found in muscle from *mdx* mice. *Nature* **335**, 735–738.

Warren GL, Hermann KM, Ingalls CP, Masselli MR & Armstrong RB (2000). Decreased EMG median frequency during a second bout of eccentric contractions. *Med Sci Sports Exerc* **32**, 820–829.

Warren GL, Ingalls CP & Armstrong RB (1998). A stimulating nerve cuff for chronic in vivo measurements of torque produced about the ankle in the mouse. *J Appl Physiol* **84**, 2171–2176.

Warren GL, Ingalls CP, Lowe DA & Armstrong RB (2001). Excitation-contraction uncoupling: major role in contraction-induced muscle injury. *Exerc Sport Sci Rev* **29**, 82–87.

Warren GL, Ingalls CP, Shah SJ & Armstrong RB (1999). Uncoupling of *in vivo* torque production from EMG in mouse muscles injured by eccentric contractions. *J Physiol* **515**, 609–619.

Warren GL, Lowe DA, Hayes DA, Karwoski CJ, Prior BM & Armstrong RB (1993). Excitation failure in eccentric contraction-induced injury of mouse soleus muscle. *J Physiol* **468**, 487–499.

Whitehead NP, Streamer M, Lusambili LI, Sachs F & Allen DG (2006). Streptomycin reduces stretch-induced membrane permeability in muscles from *mdx* mice. *Neuromuscul Disord* **16**, 845–854.

Wooddell CI, Zhang G, Griffin JB, Hegge JO, Huss T & Wolff JA (2010). Use of Evans blue dye to compare limb muscles in exercised young and old *mdx* mice. *Muscle Nerve* **41**, 487–499.

Woods CE, Novo D, DiFranco M & Vergara JL (2004). The action potential-evoked sarcoplasmic reticulum calcium release is impaired in *mdx* mouse muscle fibres. *J Physiol* **557**, 59–75.

Woods JJ & Bigland-Ritchie B (1983). Linear and non-linear EMG/force relationships in human muscles. An anatomical/functional argument for the existence of both. *Am J Phys Med* **62**, 287–299.

Yeung EW, Whitehead NP, Suchyna TM, Gottlieb PA, Sachs F & Allen DG (2005). Effects of stretch-activated channel blockers on $[Ca^{2+}]_i$ and muscle damage in the *mdx* mouse. *J Physiol* **562**, 367–380.

Additional information

Competing interests

None.

Author contributions

Conception and design of the experiments: J.A.C., G.L.W., D.A.L. Collection, analysis and interpretation of data: J.A.C., G.L.W., M.V., D.A.L. Drafting the article or revising it critically for important intellectual content: J.A.C., G.L.W., D.A.L. All experiments were carried out at the University of Minnesota.

Funding

This research was supported by grants from the NIH: K02-AG036827 (D.A.L.), P30-AR0507220 (University of Minnesota Muscular Dystrophy Center), T32-AR07612 (J.A.C.), T32-GM008244 (M.V.).

Acknowledgements

The authors would like to thank Susan A. Keirstead (University of Minnesota) for her contributions to this project.